Short title: GA-control of rice leaf length via cell division

***Author for contact**
Aashish Ranjan
National Institute of Plant Genome Research,
Aruna Asaf Ali Marg, New Delhi-110067, India
email: aranjan@nipgr.ac.in; Phone no. 91-11-26735117

Title: GA-mediated spatial control of cell division expounds the leaf size variation between cultivated and wild rice

Vikram Jathar[1], Kumud Saini[1], Ashish Chauhan[1], Ruchi Rani[1], Yasunori Ichihashi[2], Aashish Ranjan[1]*
[1]National Institute of Plant Genome Research, Aruna Asaf Ali Marg, New Delhi-110067, India.
[2]RIKEN BioResource Research Center, 3-1-1 Koyadai, Tsukuba, Ibaraki, 305-0074, Japan.

Summary: High Gibberellic Acid level promotes cell division and cell production rate in rice leaves to increase the leaf length.

Author contributions: V.J. and A.R, conceptualized the study. V.J., K.S., and A.R. designed experiments. V.J. and A.C. performed experiments. V.J., R.R., Y.I., and A.R. analyzed transcriptomic data. V.J. and K.S. analyzed leaf kinematics data. V.J. and A.R. compiled figures and wrote the manuscript. V.J., K.S. and A.R. edited the final manuscript with the contribution of all the authors. A.R. agrees to serve as the author responsible for contact and ensures communication.

Funding information: This work was supported by the core funding from the National Institute of Plant Genome Research as well as Ramalingaswamy Re-entry Fellowship (BT/RLF/Re-entry/05/2013) and Rice Network Project (BT/Ag/Network/Rice/2019-20) from the Department of Biotechnology, Ministry of Science and Technology, India.

Author for contact email: aranjan@nipgr.ac.in

Abstract

Leaf size is a major determinant of crop performance by influencing leaf physiological processes, such as light capture, transpiration, and gas exchange. Therefore, understanding the genetic basis of leaf size regulation is imperative for crop improvement. Natural variation in leaf size for a crop plant is a valuable genetic resource for a detailed understanding of leaf size regulation. We investigated the mechanism controlling the rice leaf length using cultivated and wild rice accessions that showed remarkable differences for the leaf features. Comparative transcriptomic profiling of the contrasting accessions suggested the involvement of Gibberellic Acid (GA), Growth Regulating Factor (GRF) transcription factors, and cell cycle in the rice leaf size regulation. Leaf kinematics studies showed that the increased domain of cell division activity along with a faster cell production rate drove the longer leaves in the wild rice *Oryza australiensis* compared to the cultivated varieties. Higher GA levels in the leaves of *Oryza australiensis*, and GA-induced increase in the rice leaf length via an increase in cell division zone emphasized the key role of GA in rice leaf length regulation. Zone-specific expression and silencing of the GA biosynthesis and signaling genes confirmed that OsGRF7 and OsGRF8 function downstream to GA for controlling cell cycle to determine the rice leaf length. The GA-GRF-cell cycle module for rice leaf length regulation might have contributed to optimizing leaf features during the domestication and could also be a way for plants to achieve leaf plasticity in response to the environment.

Keywords: Cultivated and wild rice, Leaf length, Leaf Kinematics, Leaf growth zones, Cell division, Gibberellic acid (GA), Growth regulatory factors (GRFs), Cyclin.

Introduction

The basic leaf development program includes leaf primordia initiation on the flanks of shoot apical meristem that follows growth and patterning by multiple transcription factor families (Townsley and Sinha, 2012; Bar and Ori, 2014; Du et al., 2018). While leaf initiation and patterning are regulated by a suite of transcription factors and complex hormonal interactions, the final leaf size – length and width – is determined by the coordination of cell division and expansion (Li et al., 2007; Gonzalez et al., 2012; Chitwood and Sinha 2016; Sarvepalli et al., 2019). Considering leaf as the major plant organ for light-harvesting and perception of environmental signals, the genetic understanding of leaf size regulation could be of paramount importance in crop improvement programs. Though leaf initiation and subsequent growth follow a similar basic program, a remarkable variation in leaf shape and size is observed within a plant species and across different species.

The regulation of leaf size is extensively studied for simple leaves of Arabidopsis and compound leaves of tomato, however detailed mechanistic studies are relatively scarce for monocot cereals except for maize (Efroni et al., 2010; Rodriguez et al., 2013; Vercruysse et al., 2020a). The spatial and temporal regulation of cell proliferation and cell elongation to determine the final leaf size varies between monocots and dicots. Cell proliferation and expansion are temporally separated in dicots as cell proliferation predominates in a young developing leaf, thereafter cells expand before reaching maturity (Beemster et al., 2005; Piazza et al., 2005; Andriankaja et al., 2012). In contrast, cell proliferation and expansion are spatially separated in monocots, such as maize, where division, elongation, and maturation zones are present together at steady-state leaf growth (Fina et al., 2017, Tardieu and Garnier 2000). Cells at the leaf base are actively dividing and smaller in size, whereas cells in the elongation zone primarily grow by expansion followed by cell maturation at the leaf tip (Granier and Tardieu, 2009). Monocot leaves with such spatial resolution of the growth zones allow the systematic study of the zones and their contribution in the leaf size control. Leaf kinematics, quantifying cell division and elongation, is a powerful tool to define a high-resolution map of leaf growth zones, and for studying the leaf growth differences across the genotypes (Sprangers et al., 2016).

Changes in the size of division and/or elongation zone alter the final leaf size in Arabidopsis and maize (Tardieu and Granier, 2000; Tardieu et al., 2000; Gonzalez et al., 2010; Kalve et al., 2014; Nelissen et al., 2018). Several phytohormones play important roles in the regulation of cell division, elongation, and transition between division and elongation (Avramova et al., 2015; Takatsuka and Umeda, 2014). The interplay of auxin and cytokinin to

103 control cell division is long established (Inze and De Veylder, 2006; Su et al., 2011). GA is
104 classically known for mediating cell-elongation response, however recent studies in
105 Arabidopsis and maize have shown its key roles in determining cell division (Achard et al.,
106 2009; Nelissen et al., 2012). GA, after being perceived by a receptor protein GIBBERELLIN
107 INSENSITIVE DWARF1 (GID1), promotes degradation of DELLA repressor proteins,
108 resulting in activation of GA-responsive transcription factors, such as GROWTH-
109 REGULATING FACTORs (GRFs) (Willige et al., 2007; Davière and Achard, 2013;
110 Omidbakhshfard et al., 2015). GRFs are reported to directly regulate cyclins to control cell
111 division in different plant species (van der Knaap et al., 2000; Choi et al., 2004; Nelissen et al.,
112 2015; Fina et al., 2017). Arabidopsis plants overexpressing, *AtGRF1*, *AtGRF2*, and *AtGRF3*
113 develop longer leaves and larger organ size, whereas *grf* mutants produce smaller and narrower
114 leaves (Kim et al., 2003; Beltramino et al., 2018). Moreover, *GRF* expression modulation in
115 maize alters leaf length with associated changes in division zone size (Wu et al., 2014; Nelissen
116 et al., 2015). Thus, GA along with downstream GRF transcription factors could be a key to the
117 genotypic differences in the leaf size across multiple accessions of a crop plant.

118 The genetic basis of leaf size differences and underlying hormonal control is poorly
119 investigated in rice. GA is known to regulate stem elongation in rice, and manipulation of GA-
120 biosynthesis and signaling genes have optimized plant height during the green revolution (van
121 der Knaap et al., 2000; Spielmeyer et al., 2002). However, a possible involvement of GA in the
122 regulation of the rice leaf size is not systematically investigated. Cultivated rice varieties along
123 with their wild relatives provide a tremendous genetic variability to study the genetic basis of
124 leaf size differences. Several wild relatives of rice accumulate higher biomass associated with
125 larger organ size including leaf size (Sanchez et al., 2013; Mathan et al., 2021). Rice
126 domestication that primarily targeted the grain features and plant architectural traits has
127 significantly reduced the genetic variability in the cultivated varieties (Huang et al., 2012; Chen
128 et al., 2021). Therefore, a comparative study of leaf size and associated growth zone differences
129 across cultivated and wild rice would provide a comprehensive understanding of genetic and
130 hormonal regulation of rice leaf size.

131 We performed detailed phenotyping of leaf features of seven cultivated varieties and
132 four wild rice accessions followed by leaf kinematics analyses of the four accessions that
133 captured the entire variation for the leaf length. RNAseq differential gene expression analysis
134 for the selected accessions suggested the major roles of phytohormones, transcription factors,
135 and cell cycle genes in determining the rice leaf size. Leaf kinematics results showed a strong
136 association of the final rice leaf length with the size of the division zone. We further attributed

137 GA-content differences and downstream transcription factors to the variation in the division
138 zone and rice leaf size between the cultivated and wild rice. Finally, silencing of GA
139 biosynthesis and signaling genes established the key role of GA and downstream signaling
140 components in controlling rice leaf size. The knowledge could be used to optimally control the
141 rice leaf growth and size for improving crop performance.
142
143 **Results**
144 **Leaf size variation across the selected cultivated and wild rice accessions**
145 Quantification of the leaf length and the maximum leaf blade width of the fully-grown
146 second to eighth leaves of the eleven rice accessions showed a strong variation in leaf length
147 and width (Supplemental Table S1). The length of fully-grown eighth leaf varied from 44.8 cm
148 in a cultivated rice *Oryza sativa ssp. indica* cv. IR64 to 87.8 cm in a wild rice *Oryza*
149 *australiensis* (Table 1). The wild rice accessions generally developed longer leaves compared
150 to the cultivated varieties. Significant variation in leaf width was also observed, with the wild
151 rice *O. latifolia* showing maximum and cultivated variety *O. sativa ssp. indica* cv. Vandana
152 showing minimum leaf width (Supplemental Table S2). We then selected four genetically
153 diverse accessions, which captured the leaf length variations across the investigated accessions,
154 for detailed phenotypic and genetic characterization. The four selected accessions were: IR64
155 (an *indica* variety of the cultivated species *O. sativa*) and Nipponbare (a *japonica* variety of
156 the cultivated species *O. sativa*) with smaller leaves, the wild rice *O. australiensis* with the
157 longest leaves, and *O. glaberrima* (the African cultivated rice) with intermediate leaf length
158 between *O. sativa* and *O. australiensis* (Table 1; Figure 1A). The leaf phenotype of second to
159 tenth leaves of the selected four accessions further confirmed the variation in leaf length pattern
160 (Figure 1B, Supplemental Figure S1). The average leaf length of a matured leaf was remarkably
161 higher for the wild rice *O. australiensis* and was moderately higher for the African cultivated
162 rice *O. glaberrima* compared to Asian cultivated varieties IR64 and Nipponbare.
163 Quantification of the leaf four lengths of the selected four accessions consistently
164 showed longer leaf in the wild rice *O. australiensis* compared to the cultivated accessions at
165 different days of emergence (Figure 1, C and D). *O. glaberrima* showed intermediate leaf
166 length between the wild rice *O. australiensis* and cultivated Asian rice varieties at different
167 days of emergence. Consistent with the leaf length, the leaf elongation rate (LER) was higher
168 for the wild rice than the cultivated accessions at different days of emergence (Figure 1E).
169 Taken together, the wild rice *O. australiensis* showed remarkably longer leaves than the

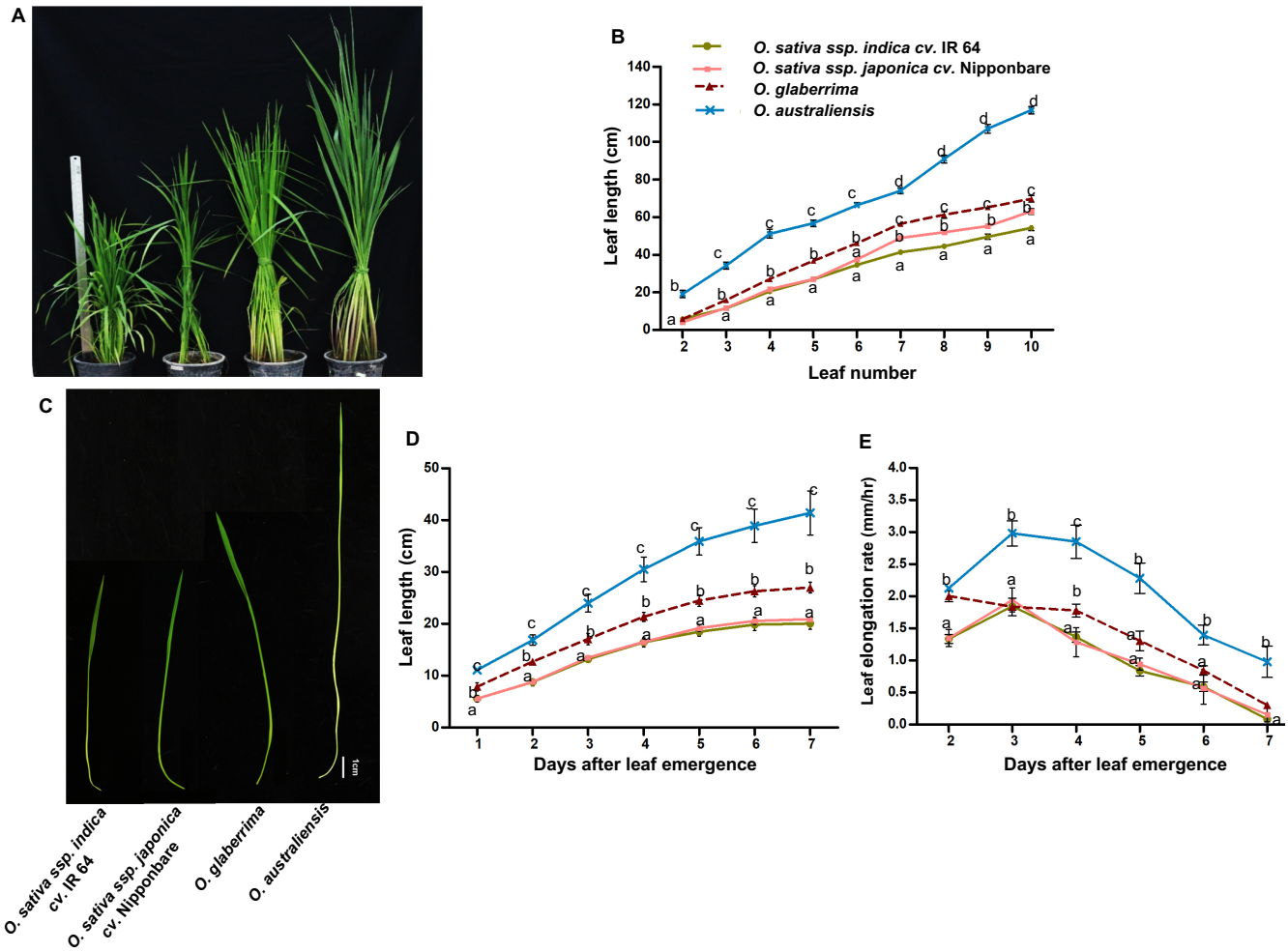

Figure 1. Wild rice *Oryza australiensis* grows longer leaf compared to the selected cultivated rice accessions. A, Representative photographs of the selected cultivated and wild rice accessions showing leaf size variations. B, Quantification of mature leaf length of leaf two to leaf ten. C, Representative leaf four images at the second day of emergence. D, Quantification of leaf four lengths at the different days of emergence. E, Leaf elongation rate of the selected rice accessions. Values in graphs represent mean±SD (n=15). Different letters indicate statistically significant differences according to one-way ANOVA followed by post-hoc Tukey HSD at $P < 0.05$.

170 cultivated varieties, and *O. glaberrima* also developed significantly longer leaves than IR64
171 and Nipponbare.
172
173 **Transcriptome profiling to identify GA and cell cycle as the key regulators of rice leaf**
174 **length**
175 To identify genes and pathways controlling the leaf length differences across the
176 selected accessions, we compared the transcriptomes of the developing fourth leaves of the
177 selected accessions on the second day after emergence. The maximum number of differentially
178 expressed genes (DEGs) was found between *O. sativa* cv. Nipponbare and *O. australiensis*,
179 whereas a lower number of DEGs was found between cultivated accessions (Supplemental
180 Table S3; Supplemental Dataset S1). Since the leaves of the wild rice *O. australiensis* were
181 remarkably longer than IR64 and Nipponbare, we first compared the gene expression profiles

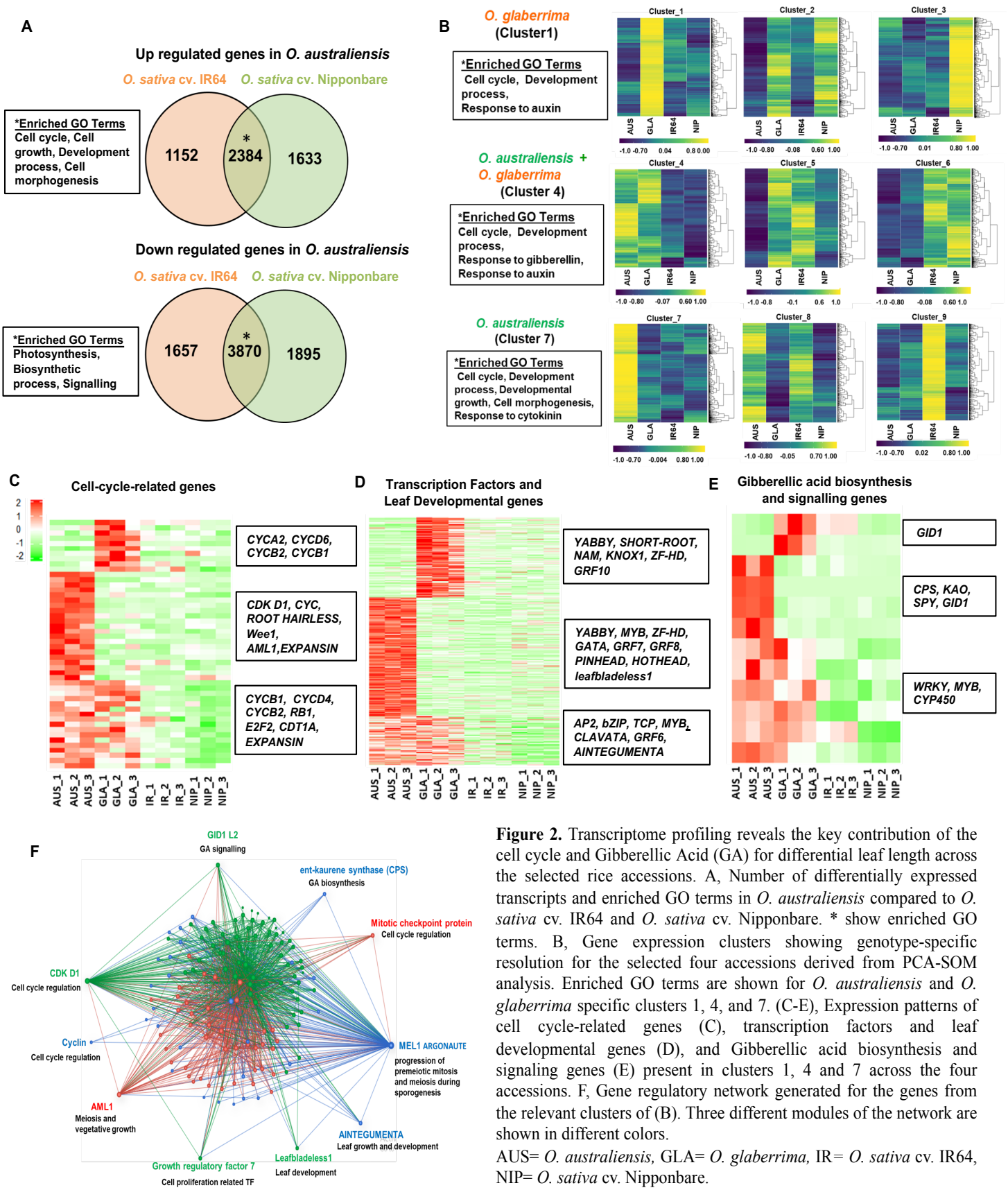

Figure 2. Transcriptome profiling reveals the key contribution of the cell cycle and Gibberellic Acid (GA) for differential leaf length across the selected rice accessions. A, Number of differentially expressed transcripts and enriched GO terms in *O. australiensis* compared to *O. sativa* cv. IR64 and *O. sativa* cv. Nipponbare. * show enriched GO terms. B, Gene expression clusters showing genotype-specific resolution for the selected four accessions derived from PCA-SOM analysis. Enriched GO terms are shown for *O. australiensis* and *O. glaberrima* specific clusters 1, 4, and 7. (C-E), Expression patterns of cell cycle-related genes (C), transcription factors and leaf developmental genes (D), and Gibberellic acid biosynthesis and signaling genes (E) present in clusters 1, 4 and 7 across the four accessions. F, Gene regulatory network generated for the genes from the relevant clusters of (B). Three different modules of the network are shown in different colors.
AUS= *O. australiensis,* GLA= *O. glaberrima,* IR= *O. sativa* cv. IR64, NIP= *O. sativa* cv. Nipponbare.

182 between the leaves of *O. australiensis* and two cultivated varieties of *O. sativa*. 2,384 genes
183 were upregulated and 3,870 genes were downregulated in growing leaves of *O. australiensis*

184 compared to both IR64 and Nipponbare (Figure 2A). The upregulated genes showed
185 enrichment of GO terms 'cell cycle', 'development process', 'cell growth', and 'cell
186 morphogenesis' (Supplemental Dataset S2). The enriched GO terms for downregulated genes
187 included 'photosynthesis', 'biosynthetic process', and 'signaling'. We also compared the gene
188 expression differences between the significantly longer leaves of *O. glaberrima* and the two
189 cultivated varieties of *O. sativa*. The 1,125 upregulated genes showed enrichment of GO terms
190 'cell cycle', 'development process', 'growth', and 'hormone transport', whereas 1,290
191 downregulated genes were enriched for the term 'metabolic process' (Supplemental Figure
192 S2A; Supplemental Dataset S2). We then analyzed the differentially expressed genes in the
193 wild rice *O. australiensis* compared to all three cultivated accessions. The 1,707 shared
194 upregulated genes in the wild rice leaves showed enrichment of GO terms "development
195 process", "cell cycle", and "growth", whereas the GO term "biosynthetic process" was enriched
196 for downregulated genes (Supplemental Figure S2B; Supplemental Dataset S2).
197 We performed principal component analysis combined with a self-organizing map
198 (PCA-SOM) to cluster the genes based on their expression pattern across the accessions.
199 Principle component 1 (PC1), explaining 75% variation in the dataset, primarily explained the
200 gene expression differences of the wild rice *O. australiensis* compared to the three cultivated
201 accessions (Supplemental Figure S3, A and B). PC2, explaining 20% of the overall variation,
202 explained the gene expression differences of *O. glaberrima* compared to the other three
203 accessions. The clusters generated by PCA-SOM provided the species-specific resolution of
204 the transcripts (Figure 2B; Supplemental Dataset S3). Since *O. australiensis* and *O. glaberrima*
205 had significantly longer leaves compared to IR64 and Nipponbare, we analyzed the genes and
206 enriched pathways in the clusters specific to either *O. australiensis* or *O. glaberrima* or both.
207 The cluster 4 that had genes specific to both *O. australiensis* and *O. glaberrima* showed
208 enrichment of terms 'cell cycle', 'development process', 'response to gibberellin', and
209 'response to auxin' (Figure 2B; Supplemental Dataset S4). The transcripts in *O. australiensis*
210 specific cluster 7 and *O. glaberrima* specific cluster 1 were enriched for 'development process'
211 and 'cell cycle'. In addition, we also found enrichment of terms related to phytohormones in
212 clusters related to *O. glaberrima* and *O. australiensis*.
213 Since transcription factors, phytohormones, and cell division and expansion are crucial
214 for leaf size regulation, we compared the expression of the related genes from the relevant
215 clusters across the selected accessions (Supplemental Dataset S5). Several cell cycle genes,
216 such as *CYCLINB, CYCLINA,* and *CDKD1*, as well cell cycle regulators, such as *E2F2* and
217 *RB1*, were expressed at higher levels in *O. australiensis* and *O. glaberrima* than IR64 and

218 Nipponbare (Figure 2C). Further, transcription factor genes known to regulate leaf growth and
219 development, such as *GRF*, *TCP*, *YAABY*, *NAM*, and *ANT*, were upregulated in *O. australiensis*
220 and *O. glaberrima* (Figure 2D). Among the genes related to phytohormones, GA biosynthesis
221 and signaling genes that included *CPS, KAO* and *GID1* were expressed at higher levels in *O.*
222 *australiensis* and *O. glaberrima* than IR64 and Nipponbare (Figure 2E). Moreover, differential
223 expressions of auxin and cytokinin biosynthesis and signaling genes were also observed across
224 the selected accessions (Supplemental Figure S3C).
225 The coexpression network of genes from the relevant clusters showed 3 major modules
226 including more than 20 nodes (Figure 2F; Supplemental Dataset S6). The network showed
227 significant connections for GA biosynthesis and signaling genes *CPS* and *GID1L2,* cell cycle-
228 related genes *CYCLIN* and *CDKD1*, as well as *GRF* transcription factor. Investigation of the
229 hub genes in module 2 showed *CDKD1* as one of the highly connected genes, which was
230 connected to GA receptor *GID1L2,* and *GRF7* (Supplemental Figure S3D). Taken together,
231 transcript profiling along with gene co-expression network highlighted cell cycle, GA, and
232 transcription factors, such as GRFs, as key contributors of rice leaf length regulation.
233
234 **Leaf kinematics to confirm the major role of cell division to regulate rice leaf length**
235 We performed DAPI staining and kinematics analyses on the growing fourth leaves to
236 investigate the differences in cell division and growth zones across the selected accessions.
237 Wild rice *O. australiensis*, with longer leaves compared to the cultivated varieties, showed
238 dividing cells for longer length from the leaf base, and thus longer division zone at different
239 days of emergence (Supplemental Figure S4A). *O. glaberrima* also showed a longer division
240 zone compared to IR64 and Nipponbare. Detailed kinematics analyses on the fourth leaves of
241 each selected accession confirmed the differences in the division zone (Figure 3; Table 2;
242 Supplemental Figure S4). All the four selected accessions showed a sigmoidal curve for
243 epidermal cell length profile, consisting of a division zone at leaf base followed by elongation
244 zone and maturation zone (Figure 3, A and B; Supplemental Figure S4, B and C). The cultivated
245 varieties Nipponbare and IR64 showed division zone extending up to 7.8mm and 7.5mm from
246 the leaf base, respectively (Figure 3, A and B, Supplemental Figure S4B). *O. australiensis*,
247 with the longest leaves, showed a remarkably longer division zone that extended to 16.7mm
248 from the leaf base (Figure 3, C and D). The longer division zone in *O. australiensis* leaves was
249 accompanied by faster cell production rate and leaf elongation rate (Table 2). *O. glaberrima*
250 also showed a longer division zone as well as a higher cell production rate compared to IR64
251 and Nipponbare (Supplemental Figure S4C). *O. australiensis* showed reasonably high overlap

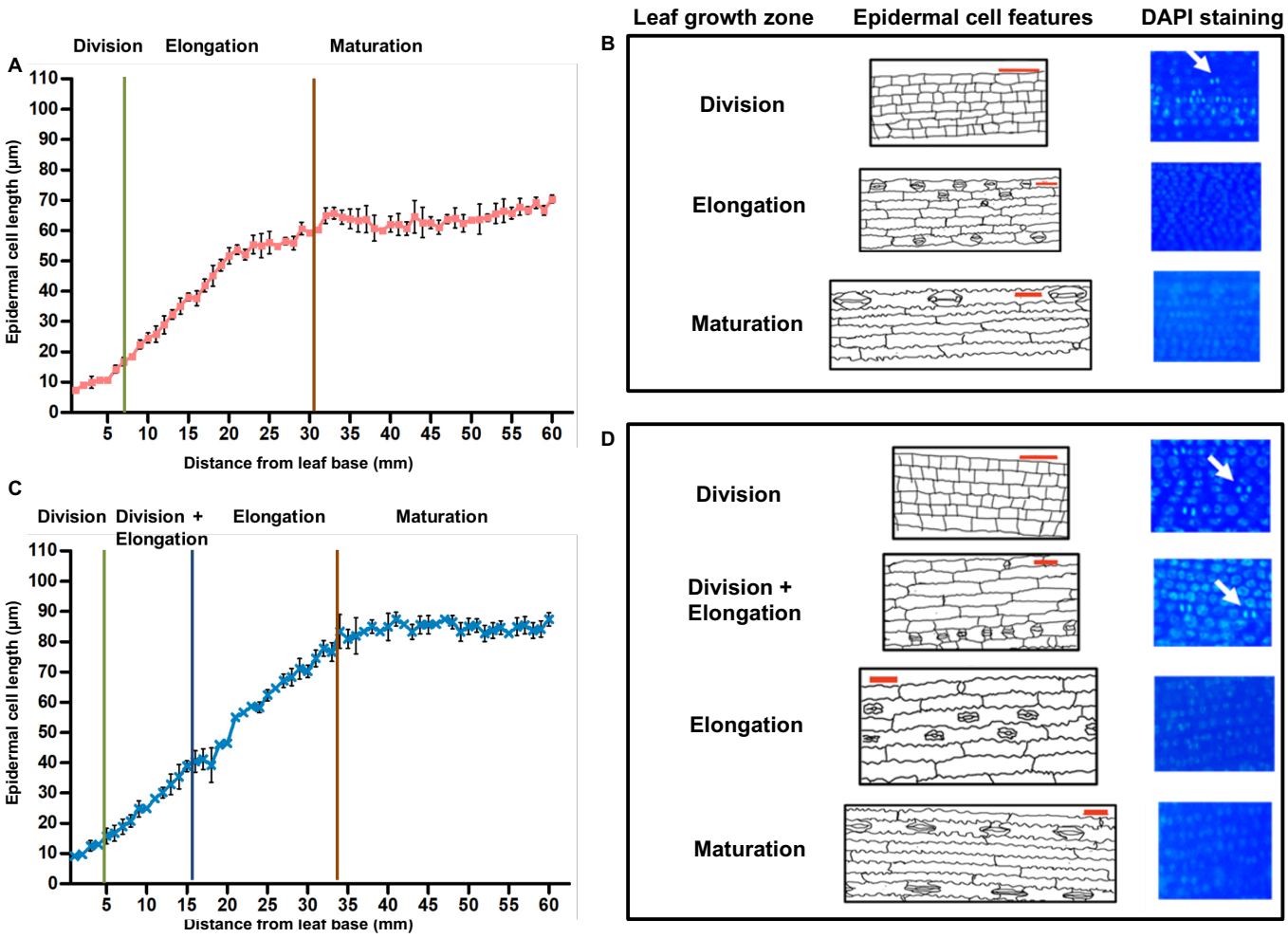

Figure 3. Leaf kinematics analyses confirm the cell division as a major regulator of rice leaf length. A, Different growth zones on leaf four of *O. sativa* cv. Nipponbare at the second day of emergence as quantified by epidermal cell length profiling and DAPI staining. B**,** Representative hand-drawn microscopic images of epidermal cells along with DAPI staining images for the different leaf-growth-zones of *O. sativa* cv. Nipponbare. C, Different growth zones on leaf four of *O. australiensis* at the second day of emergence. D, Representative hand-drawn microscopic images of epidermal cells along with DAPI staining images for the different leaf-growth-zones of *O. australiensis.* Values in A and C represent mean±SD (n=5). Vertical lines of different colors represent the separation of different leaf-growth zones. White arrows in B and D show DAPI-stained nuclei indicating dividing cells. Red scale bar = 20µm in B and D.

252 of the division zone with the elongation zone, which was not evident in the cultivated varieties
253 (Figure 3; Supplemental Figure S4).
254
255 **GA promoted cell division and the size of the division zone to increase the rice leaf length**
256 Since transcript profiling indicated the possible involvement of GA for the leaf length
257 differences across the accessions, we asked the question if GA could regulate rice leaf length
258 by controlling cell proliferation activity. To this end, we examined the effects of exogenous
259 treatment of GA_3 and GA-biosynthesis inhibitor Paclobutrazol (PAC) on leaf length and growth
260 zones of *O. australiensis* and Nipponbare. Exogenous GA_3 treatment promoted the leaf length
261 of both Nipponbare and *O. australiensis* (Figure 4, A and B; Supplemental Figure S5, A and

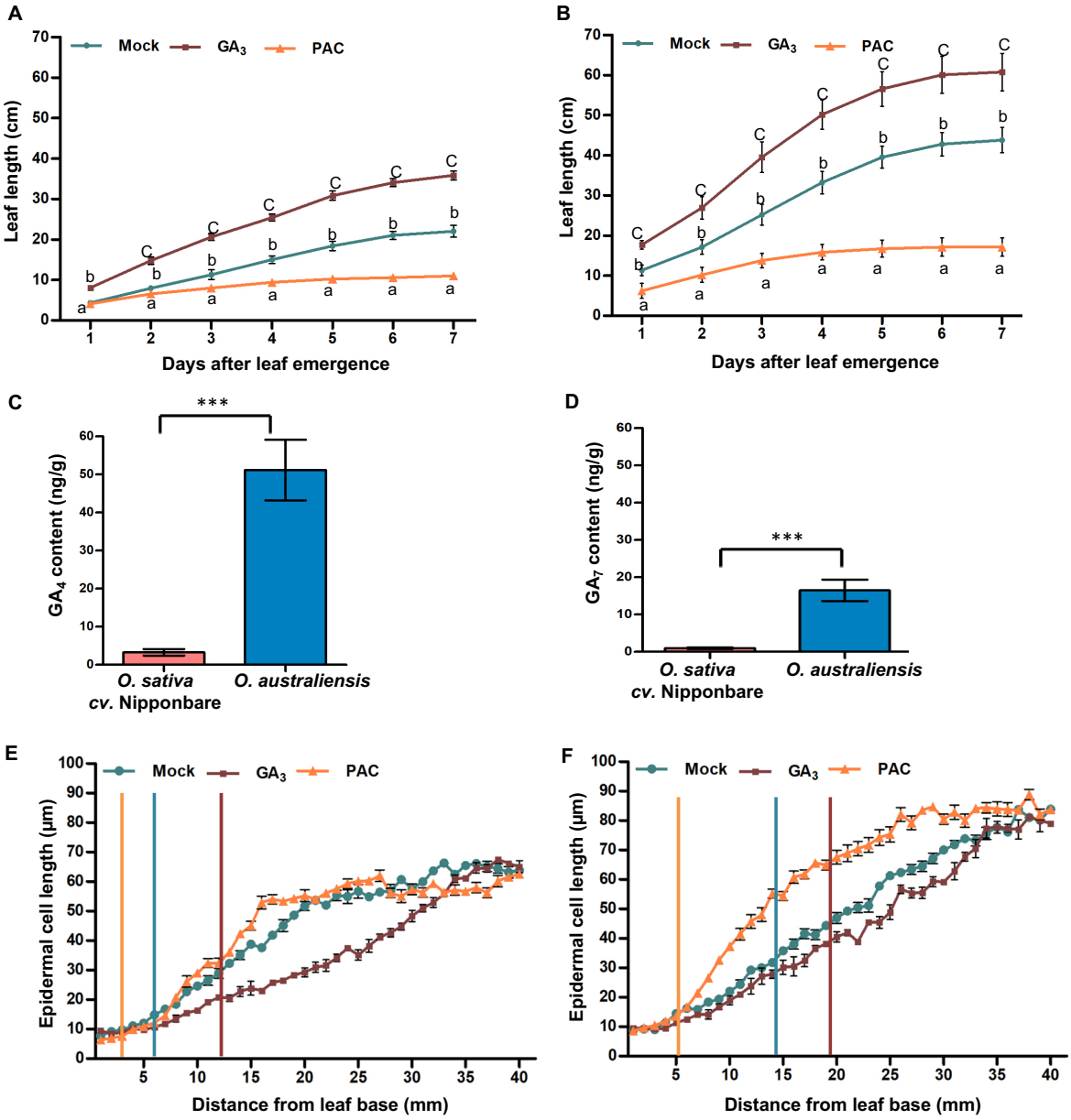

Figure 4. GA-mediated cell division control regulates the rice leaf length. (A, B), Effect of GA_3 (10μM) and Paclobutrazol (PAC, 1μM) treatments on leaf length of *O. sativa cv.* Nipponbare (A) and *O. australiensis* (B). Values represent mean±SD (n=15). Different letters indicate statistically significant differences at each day after emergence according to one-way ANOVA followed by post-hoc Tukey HSD calculation at $P < 0.05$. (C, D), GA quantification in leaf four of *O. sativa cv.* Nipponbare and *O. australiensis* at the second day of emergence. Data show mean ±SD (n=5),*** $P < 0.001$ by Student's t-test. (E, F), Different growth zones on leaf four of *O. sativa* cv. Nipponbare (E) and *O. australiensis* (F) in response to GA_3 and PAC treatments as quantified by epidermal cell length profiling and DAPI staining. Values represent mean ±SD (n=5). Vertical lines of different colors represent the size of division zones under different treatments.

B). The extent of increase in leaf length was more in Nipponbare (~1.6-fold) than *O. australiensis* (~1.3-fold). Exogenous treatment of PAC drastically reduced the leaf length of both the accessions. PAC inhibited the leaf length of Nipponbare by ~2-fold, and of *O. australiensis* by ~2.5-fold. The higher extent of increase in leaf length of Nipponbare by GA_3 treatment and higher extent of decrease in leaf length of *O. australiensis* under by PAC suggested that GA levels could be determining for the differences in the leaf length between

268 the two accessions. Higher expression of GA-biosynthesis genes in *O. australiensis* leaves than
269 Nipponbare, further, supported our hypothesis. To confirm this, we quantified GA in growing
270 fourth leaves of Nipponbare and *O. australiensis* on the second day of emergence. Consistent
271 with our hypothesis, we detected significantly higher levels of GA_4 and GA_7 in the leaves of
272 *O. australiensis* compared to Nipponbare (Figure 4, C and D).
273 To check the effects of GA on cell proliferation and division zone, we performed leaf
274 kinematics analysis on fourth leaves of *O. australiensis* and Nipponbare under GA3 and PAC
275 treatment. We observed that the leaf length promotion in response to GA treatment was due to
276 an increase in the size of the division zone in both the accessions (Figure 4, E and F;
277 Supplemental Figure S5, C and D). However, the impact of GA on cell division was more
278 striking in Nipponbare than *O. australiensis* in terms of the size of the division zone, cell
279 production rate, and the number of cells in the meristem (Supplemental Table, S4 and S5). The
280 inhibitory effect of PAC on the leaf length was also clearly due to the reduced size of the
281 division zone in both the accessions (Figure 4, E and F; Supplemental Figure S5, C and D).
282 The final epidermal cell length appeared to be similar for mock, GA treatment as well as PAC
283 treatment for both the accessions, suggesting no major effects on cell elongation. Interestingly,
284 the kinematics profile of GA-treated Nipponbare leaves resembled that of *O. australiensis*
285 leaves under control conditions with an overlap of cell division and elongation zone (Figure,
286 4E and 3C). Together the exogeneous treatment experiments and GA quantification along with
287 leaf kinematics profile in response to GA and PAC confirmed that the GA increased the rice
288 leaf length by promoting cell division and the size of the division zone.
289
290 **Growth-zone-specific expression analysis of GA-biosynthesis and signaling genes and**
291 **cell-cycle-related genes**
292 Next, we asked if zone-specific expressions of GA-related and cell cycle genes
293 contribute to leaf size differences. To this end, we quantified the expression of GA biosynthesis
294 genes in two leaf zones of Nipponbare and *O. australiensis*: zone I (leaf base – 0.8 cm; division
295 zone in both accessions) and zone II (0.8 – 1.6cm; elongation zone in Nipponbare, where
296 division extends in *O. australiensis*). The transcript levels of GA biosynthetic genes
297 *OsGA20OX2* and *OsGA3OX2* were higher in the zone I of *O. australiensis*, which showed
298 longer leaves and had higher GA levels in their leaves than Nipponbare (Figure 5, A and B).
299 Furthermore, the expression level of the GA catabolic gene *OsGA2OX4* was higher in zone II
300 of Nipponbare than *O. australiensis* (Supplemental Figure S6A). The transcript levels of
301 *OsSLR1*, encoding a GA-signalling repressor DELLA protein, was also higher in both the

302 regions of Nipponbare leaves (Supplemental Figure S6B). Taken together, higher expression
303 of GA biosynthetic genes *OsGA20OX2* and *OsGA3OX2* in the zone I, lower expression of GA
304 catabolic gene *OsGA2OX4* in zone II, and lower expression of GA-signalling repressor *OsSLR1*
305 in *O. australiensis* would promote higher GA effects in *O. australiensis* than Nipponabre.

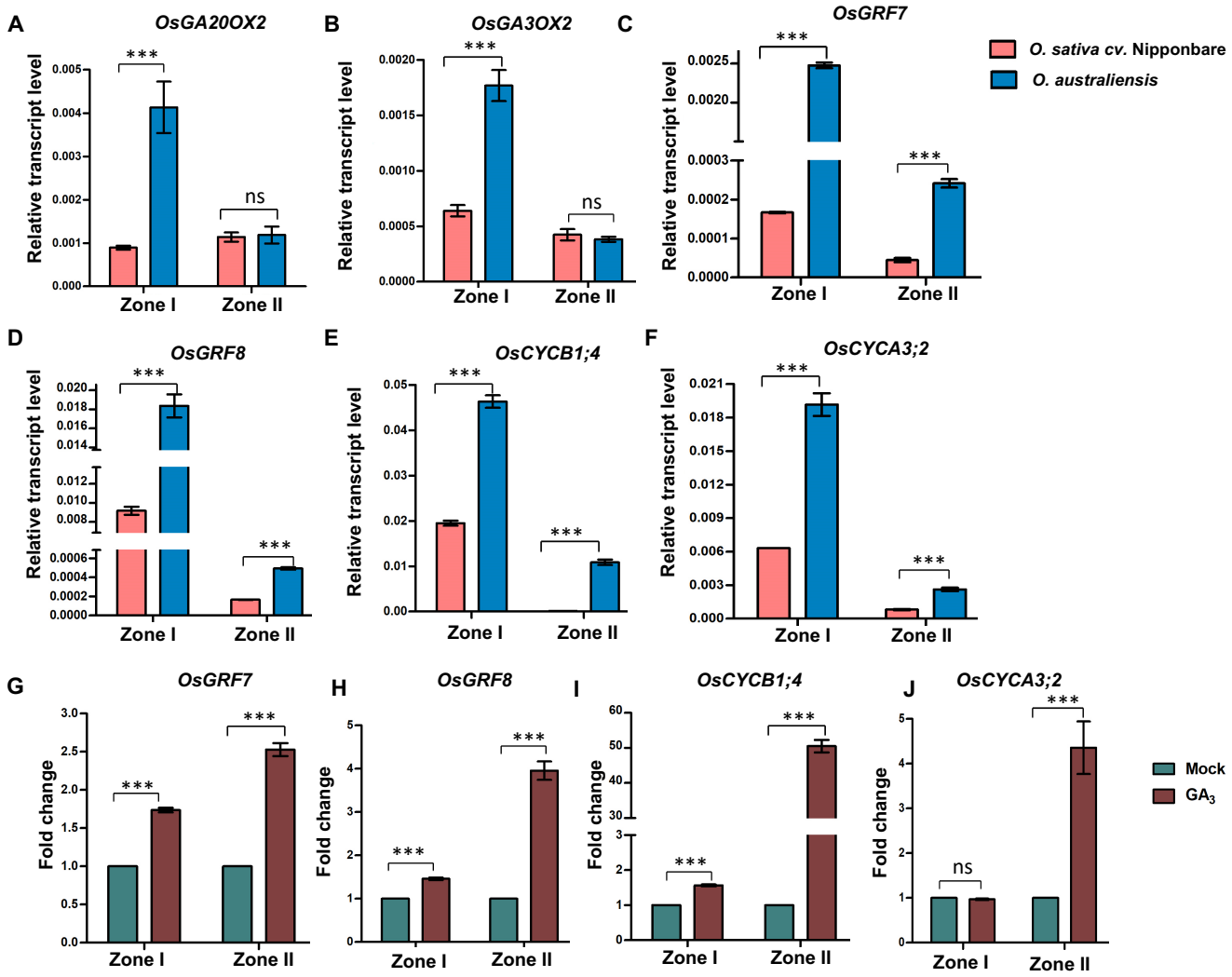

Figure 5. Zone-specific expression analysis of GA biosynthetic and signaling genes as well as cell cycle-related genes. (A-F), Expression pattern of GA biosynthesis genes *OsGA20OX2* and *OsGA3OX2* (A, B), genes encoding GRF transcription factors *OsGRF7* and *OsGRF8* (C, D), and cell cycle genes *OsCYCB1;4* and *OsCYCA3;2* (E, F) in two growth zones of *O. sativa cv.* Nipponbare and *O. australiensis*. Zone I represents the region from leaf base to 0.8cm and zone II represents 0.8cm to 1.6cm from the leaf base. (G-J), Effect of GA_3 treatment on the expression of *OsGRF7* (G), *OsGRF8* (H), *OsCYCB1;4* (I), and *OsCYCA3;2* (J) in the two growth zones of *O. sativa cv.* Nipponbare. Data shown are mean ±SD of three biological replicates, *** $P < 0.001$ by Student's t-test.

306 We checked the growth-zone-specific expressions of genes encoding GRF transcription
307 factors and cyclins. Similar to the expression of GA-biosynthesis and signaling genes, we
308 observed remarkably higher transcript levels of *OsGRF7* and *OsGRF8* in both zones I and II
309 of *O. australiensis* leaves compared to Nipponbare (Figure 5, C and D). The transcript levels
310 of *OsCYCB1;4* and *OsCYCA3;2* were also higher in both zone I and II of the *O. australiensis*

311 than Nipponbare (Figure 5, E and F). Limited transcript levels of *OsCYCB1;4* and *OsCYCA3;2*
312 in zone II of Nipponbare leaves matched with the negligible cell division activity beyond 0.8cm
313 in the accession. The significantly lower expression level of cell cycle inhibitor *OsKRP4* and a
314 higher level of cell cycle activator *OsE2F2* in basal regions of *O. australiensis* leaves than
315 Nipponbare further reflected on the differences in cell cycle between the two accessions
316 (Supplemental Figure S6, C and D). We then asked the question of whether a GA-mediated
317 increase in the size of the division zone and leaf length of Nipponbare involved GRFs and
318 cyclins. The exogenous GA treatment remarkably induced the expression levels of *OsGRF7*
319 and *OsGRF8* as well as *OsCYCB1;4* and *OsCYCA3;2* in zone II of Nipponbare, leading to the
320 increased size of the division zone (Figure 5, G-J). Treatment of GA-biosynthesis inhibitor
321 PAC led to significant suppression of the expressions of *GRF*s and *CYCLIN*s in the division
322 zone of Nipponbare (Supplemental Figure S6E). Together, gene expression analyses in
323 different zones of the two contrasting accessions as well as in response to the exogenous GA
324 treatment strongly supported our hypothesis of GA-mediated cell cycle control through GRFs
325 to determine the rice leaf length.
326
327 **Silencing of GA biosynthesis and signaling genes to confirm the GA-mediated regulation**
328 **of rice leaf length**
329 To confirm the roles of GA biosynthesis and signaling in rice leaf length regulation, we
330 performed transient silencing of genes encoding a GA biosynthesis enzyme OsGA20OX2, a
331 GA signaling repressor OsSLR1, and a GA-responsive transcription factor OsGRF7 in
332 Nipponbare. These genes were selected based on transcriptomic comparisons as well as zone-
333 specific quantification of expression levels. Silencing of *OsGA20OX2* led to a reduction in leaf
334 length of Nipponbare, similar to exogenous PAC treatment (Figure 6, A and B; Supplemental
335 Figure S5A). The reduction in leaf length of the silenced lines was associated with reduced size
336 of the division zone as well as lower expression levels of *GRF*s and *CYCLIN*s than the control
337 (Figure 6, B and C). In contrast, silencing of *OsSLR* led to a longer leaf length, increased size
338 of division zone, and higher expression levels of *GRF*s and *CYCLIN*s compared to the control
339 (Supplemental Figure S7, C and E). Similar to *OsGA20OX2*, silencing of *OsGRF7* also reduced
340 the Nipponbare leaf length along with the smaller size of the division zone and reduced
341 expression of downstream *CYCLIN* genes (Figure 6, D-F). Together, leaf phenotypes of these
342 silencing lines confirmed the GA-mediated regulation of cell division zone through GRF
343 transcription factors to determine the rice leaf length.
344

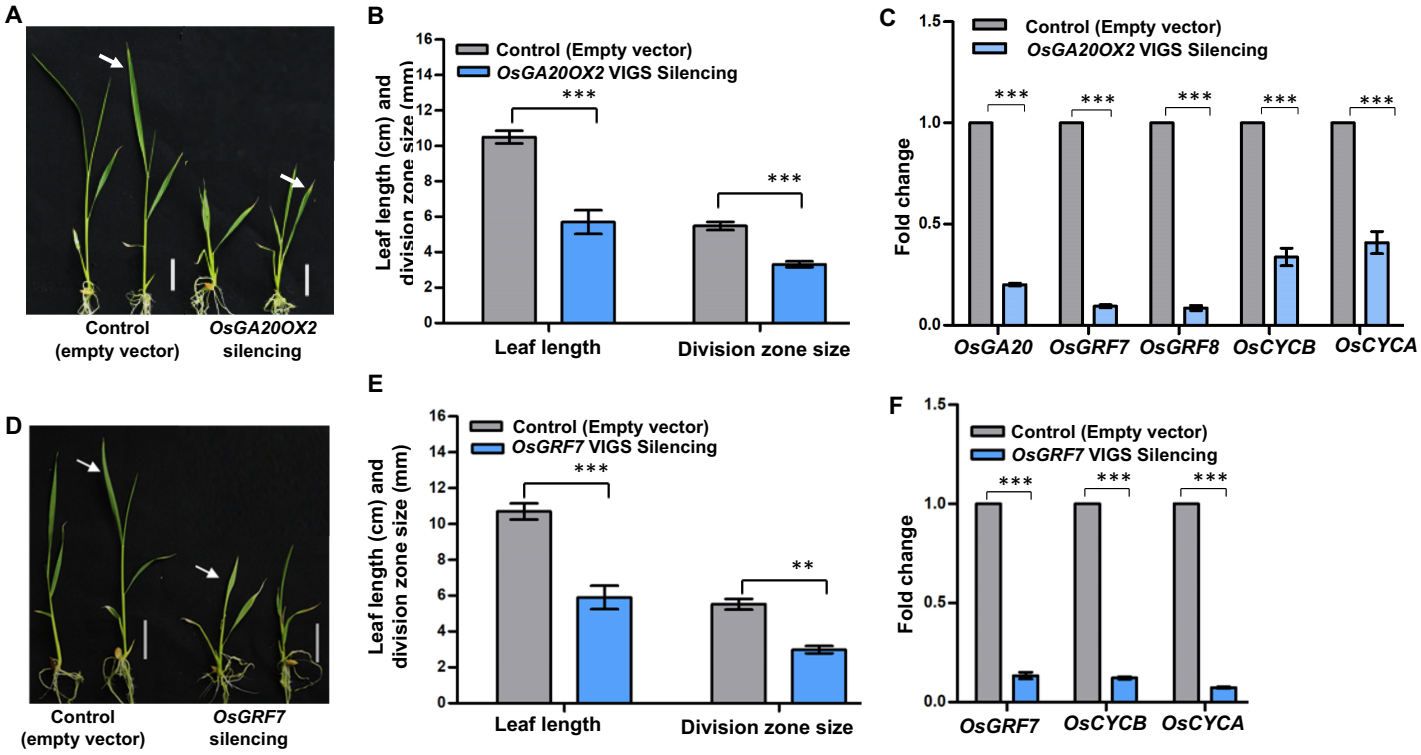

Figure 6. The silencing of GA-related genes confirms the GA-mediated regulation of rice leaf length. A, Shown are the leaf phenotypes of *OsGA20OX2* silencing in *O. sativa cv.* Nipponbare along with the control plants. B, Effect of *OsGA20OX2* silencing on leaf length and size of division zone. C, Expression levels of target GA biosynthetic gene, *GRFs*, and *CYCLINs* in *OsGA20OX2* silencing lines. D, Shown are the leaf phenotypes of *OsGRF7* silencing in *O. sativa cv.* Nipponbare along with the control plants. E, Effect of *OsGRF7* silencing on leaf length and size of division zone. F, Expression analysis of target *GRF7* and *CYCLINs* in *OsGRF7* silencing lines. Data represent mean ±SD of at least three biological replicates, *** $P < 0.001$ and ** $P < 0.01$ by Student's t-test.

Discussion

Detailed genetic understanding of the leaf size regulation is important for crop improvement programs, as leaf size strongly influences physiological processes, such as light capture efficiency, transpiration, and gas exchange (Zhu et al., 2010). Natural variation for the leaf size in a crop species and related wild accessions is an excellent resource for understanding the genetic and hormonal basis of leaf size regulation. Since crop plants, such as rice, have significantly lost the genetic variability for many desirable agronomic traits during the domestication, inclusion of wild relatives for a comparative study with cultivated crop varieties would provide a comprehensive genetic basis of leaf size changes (Huang et al., 2012; Chen et al., 2021). Studies have reported remarkable variations in the leaf morphological and anatomical features across cultivated and wild species of genus *Oryza*, suggesting a strong genetic control on leaf features of rice (Chatterjee et al., 2016; Mathan et al., 2021). We selected four rice accessions, based on detailed leaf size phenotyping of eleven accessions, that not only represented a significant genetic diversity but also covered the entire range of leaf length

359 variations among the investigated accessions for detailed mechanistic studies. Consistent with
360 the genetic differences, the transcriptome profile of wild rice *O. australiensis* was significantly
361 different from the cultivated accessions, resulting in a higher number of differentially expressed
362 genes for the wild rice and cultivated rice comparisons than between the cultivated accessions.
363 Nonetheless, we detected basic leaf developmental, phytohormonal, and transcription factor
364 genes, though at different expression levels, suggesting the conserved nature of these genes
365 across the selected accessions.

366 Differences in the leaf length are attributed to basic cellular features and leaf
367 developmental programing (Gonzalez et al., 2012; Kierzkowski et al., 2019). Consistent with
368 this, cell cycle and development were the obvious enriched terms for the genes expressed at
369 higher levels in the accessions with longer leaves. Detailed leaf kinematics analyses for the
370 contrasting cultivated and wild rice accessions precisely established the predominant role of
371 cell division activity for defining the rice leaf length. Higher cell production rate and extension
372 of cell division to an extended length from leaf base drove the longer leaf phenotype in the wild
373 rice *O. asutraliensis* than the cultivated varieties (Figure 3; Table 2). Cell cycle duration and
374 cell division rate were comparable across the accessions, suggesting that the longer cell
375 division zone and increased cell production rate at the leaf base resulted in the production of a
376 higher number of cells that contributed to long-sized leaf in the wild rice. Higher expression
377 levels of genes encoding cyclins and cyclin-dependent kinases in the growing leaves of the *O.*
378 *asutraliensis* from the comparative transcriptome profiling along with zone-specific expression
379 analysis showing higher and expanded domain of *CYCLIN*s expression in *O. asutraliensis* than
380 the cultivated variety further supported the key importance of the cell division activity for the
381 rice leaf length regulation (Figure 2C; Figure 5, E and F). *O. asutraliensis*, besides showing
382 the expansion of the division zone, showed longer epidermal cell compared to cultivated
383 varieties, suggesting that the cell elongation also contributes to the longer leaf length of the
384 wild rice (Figure 3C).

385 Spatial and temporal regulation of cell division activity in plants is under complex
386 regulation of phytohormones and transcription factors (Nelissen et al., 2012; Takatsuka and
387 Umeda, 2014). We detected auxin-, cytokinin-, and GA-related genes among the differentially
388 expressed genes for the selected rice accessions. Besides, genes encoding transcription factors
389 known to regulate cell division, such as GRFs and TCPs, were also differentially expressed
390 between the contrasting rice accessions (Figure S3C; Vercruysse et al., 2020b). GA is shown
391 to control the cell division activity via the involvement of GRF transcription factors in
392 Arabidopsis and maize (Lantzouni et al., 2020; Fina et al., 2017). Our comparative

393 transcriptome profiling showed higher expression of GA-biosynthesis and signaling genes as
394 well as GRF transcription factors in the longer leaves of *O. australiensis* and *O. glaberrima*
395 than IR64 and Nipponbare, suggesting the key functions of GA and GRF transcription factors
396 to regulate cell division activity for differential leaf length across the selected accessions
397 (Figure 2, D and E). Therefore, we hypothesized the GA-GRF-cell cycle as a key module not
398 only as a general regulator of rice leaf length but also for attenuating the leaf size during the
399 domestication. The differentially expressed auxin- and cytokinin-related genes attest to the
400 fine-tuning of leaf size and other leaf features through the coordinated functions of multiple
401 different phytohormones. Differential expression of many leaf developmental genes across the
402 rice accessions would likely explain the extensive leaf patterning and differentiation
403 differences across different cultivated and wild rice.

404 GA is reported to be involved in the maintenance of the division zone size and
405 accumulates in the transition zone in maize (Nelissen et al., 2012). In support of the GA-GRF-
406 cell cycle module to regulate rice leaf length, growing leaves of *O. australeinsis* had higher
407 levels of bioactive GAs than Nipponbare that would promote the size of the division zone
408 extending into the elongation zone, leading to a significantly enlarged transition zone in the
409 wild rice (Figure 4, C and D). Higher expression levels of GA biosynthesis genes *OsGA20OX2*
410 and *OsGA3OX2* in the basal division zone of *O. australeinsis* leaves than Nipponbare
411 corroborated the higher GA content in the wild rice (Figure 5, A and B). In addition, lower
412 expression of GA-catabolic gene *OsGA2OX4* in the transition zone of the wild rice than
413 Nipponbare likely maintained higher GA levels in the zone. Consistent with these, exogenous
414 GA-treatment increased the rice leaf length by extending the zone where cell division operates.
415 GA is known to induce cell elongation response (Jones and Kaufman, 1983). Exogenous GA-
416 treatment, however, increased the leaf length without altering the mature epidermal cell length,
417 suggesting that GA primarily affects rice leaf length via regulation of cell division
418 (Supplemental Table S4 and S5). The longer epidermal cells of *O. australeinsis*, thus, could
419 likely be attributed to the functions of other phytohormones. Finally, reduction in rice leaf
420 length by silencing *OsGA20OX2* that involved downregulation of *CYCLIN*s confirmed the
421 central role of GA in rice leaf length regulation through cell division control (Figure 6, A-C).

422 GRF transcription factors promote cell division activity by directly binding to the
423 promoters of *CYCA1;1* and *CDC20* (Li et al., 2018). Moreover, GRF7 regulation of GA-
424 biosynthesis and auxin-signaling genes control the rice plant architecture (Chen et al., 2020).
425 Higher *GRF7* and *GRF8* expression in growing leaves of rice accessions with longer leaves
426 from RNAseq analysis along with more *GRF7* and *GRF8* transcripts in division and transition

427 zones of *O. australeisnsis* than Nipponbare suggested that GRF7 and GRF8 may connect GA-
428 levels and cell cycle for rice leaf size regulation (Figure 5, C and D). GA-treatment, increasing
429 the leaf length by increasing the domain of cell division, induced the *GRF7* and *GRF8*
430 expression in both division and transition zone, further, suggesting the GRF7 and GRF8
431 functions downstream to GA (Figure 5, G-J). Consistent with this, silencing of *GRF7* resulted
432 in reduced rice leaf length with an associated decrease in the expression of the *CYCLIN*s
433 (Figure 6, D-F). Silencing of *OsSLR1*, a DELLA protein that inhibits GRF functions to repress
434 GA signaling, led to increased leaf length along with higher expression of *GRF7* and *GRF8*,
435 further supporting the functions of GRF7 and GRF8 to integrate GA levels and leaf length
436 regulation.

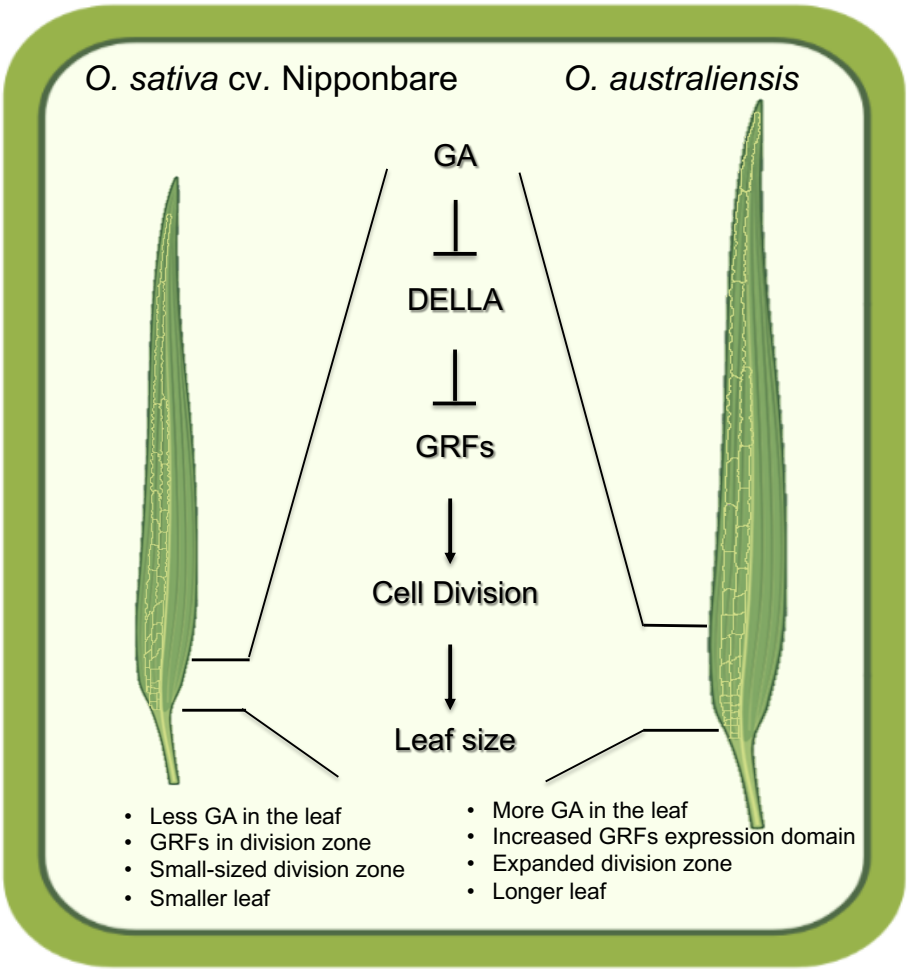

Figure 7. The GA-GRF-cell cycle module is a key regulator of the rice leaf length control. GA-mediated induction in the expression domain of GRF transcription factors expands the region with cyclin expression at the leaf base, thus promoting the longer division zone with a higher cell production rate leading to longer leaves in rice. Higher GA levels and downstream signaling resulting in increased cell division activity explained the longer leaves of the wild rice *O. australiensis* compared to the cultivated varieties.

437 In conclusion, we showed that the GA-regulated cell proliferation controls the final rice
438 leaf length and explains the variation in leaf length across diverse rice accessions (Figure 7).

439 Comparative transcriptomic profiling along with gene-coexpression networks suggested the
440 key roles of GA, GRF transcription factors, and cell cycle for rice leaf length regulation. Leaf
441 kinematics and GA experiments further strengthened the hypothesis of GA-mediated leaf
442 length regulation via cell division control. Zone-specific expression analysis and silencing of
443 candidate GA biosynthesis and signaling genes confirmed that the GA-mediated cell division
444 control to regulate leaf length involves downstream GRFs. Taken together, higher GA levels
445 and associated downstream components resulting in increased cell division activity explained
446 the long leaves of the wild rice *O. australiensis* compared to the cultivated varieties (Figure 7).
447 The established GA-GRF-cell cycle module could not only be a general regulator of rice leaf
448 length but also have contributed to the optimization of leaf size during domestication. The
449 module could, further, be a way for plants to achieve cellular plasticity in response to their
450 growth environment.
451
452 **Materials and Methods**
453 **Plant materials and growth conditions**
454 The genotypes used for this study are summarized in Supplementary Table S1. Rice seeds were
455 first germinated on Petri plates containing wet germination paper for 7 days, followed by
456 transfer of germinated seedlings to a hydroponic solution containing one fourth MS Media
457 (Himedia) with micro and macronutrients in standard concentrations. The nutrient solution was
458 changed every third day during the seedling growth. Seedlings were grown in a greenhouse at
459 28 ºC day and 23 ºC night temperature with 14:10 hours of light and dark cycle. For exogenous
460 GA and GA-biosynthesis inhibitor treatment experiments, 10μM of gibberellic acid (GA3),
461 and 1μM of gibberellic acid biosynthesis inhibitor PAC (paclobutrazol) were directly added in
462 hydroponic solution.
463
464 **Phenotyping of leaf morphological traits and leaf growth analysis**
465 The quantification of leaf length and width was performed on each individual fully-grown leaf
466 from second to eight leaves of all the selected cultivated and wild rice accessions. Leaf length
467 and width were quantified manually using a ruler. Leaf-sheath length was measured as a
468 distance between the seedling base to ligule. The leaf-blade length was quantified as the
469 distance between the ligule to the leaf tip. Leaf-blade width was measured in the central widest
470 part of the fully expanded leaf blade. Total mature leaf length was calculated by adding leaf
471 sheath and leaf blade length. The leaf growth analysis was done on leaf four, when the leaf
472 emerged from the sheath of the third leaf, as explained by Sprangers et al. (2016). Leaf length

473 was measured daily from the day of emergence up to the seventh day by considering the
474 seedling base as the starting point of the leaf. The time of emergence of the fourth leaf varied
475 from species to species (around 10 days in *O. sativa* cv. IR64 and Nipponbare, 12 days in
476 African cultivated rice *O. glabberrima*, and 18-19 days in the wild rice *O. australiensis* after
477 germination). Leaf elongation rate (LER) was calculated as the leaf growth in one day divided
478 by the time interval. For this, the leaf length was quantified at specific time points on each day.
479 All the quantifications were performed using at least 15 individual plants of each accession.
480

481 **RNA-seq library preparation and sequencing**

482 Leaf four of the selected accessions were collected at the same developmental stage (48 hrs.
483 after leaf emergence when the leaves are growing at a steady growth rate) for RNA-seq library
484 preparation. Libraries were prepared in three biological replicates using YourSeq Full
485 Transcript RNAseq Library Kit (AMARYLLIS NUCLEICS) as per the manufacturer's
486 protocol. These RNA-seq libraries were sequenced on the Illumina HiSeq platform, and reads
487 were generated in 150bp paired-end format.
488

489 **Quality filtering, mapping of reads, and differential gene expression analysis**

490 The reads were quality filtered using the NGSQC toolkit that involved removal of adapter
491 sequences and low-quality reads (Phred score <30) (Patel et al., 2012). The quality-filtered
492 reads were then mapped to reference coding DNA sequences (CDS) of rice from the Rice
493 Genome Annotation Project database (RGAP 7) using default parameters of bowtie2
494 (Langmead and Salzberg, 2012). SAMtools were used to generate bam alignment files that
495 were used to tabulate raw counts for each gene (Li et al., 2009). edgeR was used for differential
496 gene expression analysis (Robinson et al., 2010). Genes for which there were 2 or fewer cpm
497 in less than three replicates were not considered further. glm approach with quasi-likelihood F-
498 test was used for differential gene expression analysis. Significant differences in gene
499 expression levels for different pair-wise comparisons were determined based on FDR cut-off
500 < 0.05 and logFC value >1 and <-1.
501

502 **Principle Component Analysis with Self Organizing Map (PCA-SOM) clustering**

503 Normalized read counts (Supplemental Data Set S7) were used for a gene expression clustering
504 method (Chitwood et al., 2013). For clustering, the genes in the upper 50% quartile of
505 coefficient of variation for expression across different species were used. The scaled expression
506 values were used to generate species-specific gene clusters (Wehrens and Buydens, 2007).

507 Three by three hexagonal SOM clusters and 100 training interactions were used during
508 clustering. The SOM clusters were visualized in PCA space, where PC values were calculated
509 based on gene expression across the species with the help of the prcomp R package. The
510 heatmaps were generated for each cluster using superheat R package.
511
512 **GO Enrichment Analysis**
513 GO enrichment analysis of the differentially expressed genes as well as for genes present in
514 each PCA-SOM cluster was performed using the Plant Transcriptional Regulatory Map GO
515 enrichment tool of Plant Transcription Factor Database (Tian et al., 2019).
516
517 **Gene regulatory network analysis**
518 An unsigned correlation network was constructed using the weighted gene correlation network
519 (WGCNA) package version 1.68 (Langfelder et al., 2008). Data were z-score normalized (R
520 scale function). The soft-thresholding power was chosen based on a scale-free topology with a
521 fit index of 0.8. An adjacency matrix with the selected soft-thresholding power was calculated
522 and transformed into a topological overlap matrix (TOM). Using the TOM, network properties
523 such as strength were calculated and the network was visualized using the igraph package
524 version 1.2.5 (Csardi et al., 2006) and visNetwork 2.0.9 (https://datastorm-
525 open.github.io/visNetwork/). A Fast-Greedy modularity optimization algorithm was selected
526 to define modules in the integrated network.
527
528 **Leaf kinematics analysis**
529 Leaf kinematics analysis was performed as described by Sprangers et al. (2016). To estimate
530 the size of division zone size, the basal 4 cm segment of leaf four was collected from each
531 accession at different days of emergence up to day five. Samples were placed in 3:1 (v/v)
532 absolute ethanol: acetic acid for fixation of cell walls and clearing of chlorophyll, rinsed for 30
533 min in a buffer containing 50 mM NaCl, 5 mM EDTA, and 10 mM Tris-HCl, pH 7, and nuclei
534 were stained by incubating the samples in the dark for 2 min in the same buffer solution
535 containing 49,6-diamino-phenylindole (DAPI) at a concentration of 1 mg/ml. Fluorescent
536 nuclei were observed with a microscope equipped with an epi-fluorescent condenser (Nikon
537 80i-epifluorescence Microscope), and the images obtained were used to measure the size of the
538 division zone as the distance between the base of the leaf and the most distal mitotic cell. To
539 determine cell length profiles, leaf four was collected on the second day after leaf emergence
540 at the steady-state growth, and prepared for microscopy. The collected leaves were initially

541 kept in absolute ethanol for 48 h (ethanol changed once after 24 h), and then transferred to
542 lactic acid and stored at 4°C. Samples were mounted on microscope slides using glycerol as a
543 mounting medium, and then successive images were taken using a bright field microscope
544 (LMI, UK). Leaf kinematics analyses for GA- or PAC- treated seedlings were also performed
545 as explained above. The various growth parameters from the leaf kinematics experiments were
546 quantified using formulae explained in Sprangers et al. (2016).
547
548 **Gibberellic acid (GA) quantification**
549 200-250 mg of fresh leaves tissue at the second day of emergence at steady-state growth, when
550 leaf kinematics and transcriptomics were also performed, were collected and finely ground in
551 liquid nitrogen. The samples were extracted in ice-cold buffer (MeOH: H2O: HCOOH,
552 15:4:0.1) on a shaker for overnight at 4°C. Then internal standard was added in the extract and
553 vortexed for 10 min. The extract was centrifuged for 15 min at 16,000 rcf at 4°C. Then the
554 supernatant was passed onto a pre-conditioned (MeOH and 0.1% of HCOOH) C18 RP SPE
555 column. The column was washed with 0.1% HCOOH and 5% MeOH. Finally, elution was
556 done with ice-cold 0.1% HCOOH in Acetonitrile. After evaporation of the solvent, the pellet
557 was re-suspended in 5% MeOH. GA content was then analyzed using LC-MS/MS.
558
559 **RNA isolation, cDNA synthesis, and qRT-PCR analysis**
560 After defining growth zones on leaf 4, samples for expression profiling were collected
561 according to the length of a specific zone. Total RNA was isolated using Trizol reagent
562 (Invitrogen) as described by Longeman et al. (1987) and treated with RNase-free DNase I
563 (Thermo Fisher Scientific). 1.5 µg of total RNA was reverse transcribed to first-strand cDNA
564 using RevertAid First-Strand cDNA Synthesis Kit (Thermo Fisher Scientific) following the
565 manufacturer's instructions. The quantitative real-time-PCR (qRT-PCR) analysis was
566 performed on the CFX Connect Real-Time System (Bio-rad) using PowerUp™ SYBR® Green
567 fluorescence dye (Thermo Fisher Scientific). The primer pairs for qRT-PCR were designed
568 based on gene sequences obtained from RGAP 7 (Rice Genome Annotation Project database)
569 (Supplemental Table S6). The primer efficiency analyzed using a standard curve method. From
570 each species five different cDNA concentration (25,50,100,200 and 400ng) used to generate
571 standard curve and primer efficiency was calculated using the formula E = (10[-1/slope] 257 -
572 1) *100. The primer specificity of amplified gene products across the selected rice genotypes
573 was viewed through dissociation curve analysis. Relative expressions of the target genes were
574 analyzed using actin (LOC_Os03g50885.1) as the internal control applying the $2^{-\Delta\Delta Ct}$ method

575 for fold change and $2^{-\Delta Ct}$ method for relative transcript levels quantification (Livak and
576 Schmittgen 2001). The expression pattern of each gene was confirmed by the independent
577 biological experiments.
578
579 **Transient gene silencing line generation**
580 Virus-induced gene silencing (VIGS) mediated transient silencing line for *OsGA20OX2,*
581 *OsGRF7,* and *OsSLR1* genes were generated using the mVIGS vector as previously described
582 by Kant et al. (2017). In short, recombinant vector constructs were transformed into
583 Agrobacterium strain EHA105, and a single Agrobacterium colony was used to initiate a
584 primary culture in LB medium supplemented with kanamycin and rifamycin antibiotics. After
585 overnight incubation at 28 ºC, a secondary culture was grown to an OD600 of 0.6 to 0.8 with
586 200 µM acetosyringone. Cells were harvested after centrifugation and resuspended in 10 mM
587 MES, 10 mM MgCl2, and 200 µM acetosyringone. 6-day old rice seedlings were injected with
588 50 µL of bacterial suspension into the meristematic region located at the basal region of
589 seedlings. After Agro-inoculation seedlings were transferred onto sterile Whatman No. 1 filter
590 paper immersed in MS medium placed on a solid support with its ends dipped into a reservoir
591 containing the nutrient medium. To avoid drying, plant roots were covered with moist tissue
592 paper and transferred to tubes containing MS medium 24 h post-inoculation and were
593 maintained at 28°C under conditions described above. Transgenic seedlings were screened
594 based on expression analysis of target genes as well as based on leaf morphological differences.
595 As a positive control, we generated a transient silencing line for chlorophyll biosynthesis gene
596 (*ChlH*) and confirmed positive transgenic plants by observing leaves chlorosis phenotype and
597 gene expression analysis (Supplemental Figure S7, A and B).
598
599 **Accession Numbers**
600 The quality-filtered reads, which were used to get the normalized read counts and for DE
601 analysis, were deposited to the NCBI Short Read Archive under accessions SRRXXXXXXX
602 to SRRXXXXXXX.
603
604
605
606
607
608

609 **Supplemental Data**

610 **Supplemental Figure S1.** Leaf length and width phenotyping of the four selected accessions.

611

612 **Supplemental Figure S2.** Differentially expressed transcripts and enriched GO terms in *O.*
613 *glaberrima* and *O. australiensis*.

614

615 **Supplemental Figure S3.** PCA-SOM clustering of gene expression across the selected rice
616 accessions.

617

618 **Supplemental Figure S4.** Cellular basis of leaf size differences across the selected rice
619 accessions.

620

621 **Supplemental Figure S5.** Effects of GA and paclobutrazol treatments on leaf length and
622 division zone size.

623

624 **Supplemental Figure S6.** Zone-specific expression analysis of GA- and cell cycle-related
625 genes.

626

627 **Supplemental Figure S7.** Silencing of positive control *OsChlH* and *OsSLR1,* a GA-signalling
628 repressor.

629

630 **Supplemental Table S1.** List of cultivated and wild rice accessions used in the present study

631

632 **Supplemental Table S2.** Quantification of maximum leaf width of fully-developed leaves of
633 the seven cultivated and four wild rice accessions.

634

635 **Supplemental Table S3.** The total number of differentially expressed genes along with
636 upregulated and downregulated genes for each pair-wise comparison.

637

638 **Supplemental Table S4.** Quantification of leaf kinematics parameters of the growing leaf
639 four of *O. sativa* cv. Nipponbare under exogenous GA_3 and paclobutrazol treatments.

640

641 **Supplemental Table S5.** Quantification of leaf kinematics parameters of the growing leaf
642 four of *O. australiensis* under exogenous GA_3 and paclobutrazol treatments.

643

644 **Supplemental Table S6.** List of primers used for gene expression analysis and transient
645 silencing experiments.

646

647 **Supplemental Dataset S1**. List of statistically significant differentially expressed genes for
648 each pair-wise comparison.

649

650 **Supplemental Dataset S2.** List of statistically significant GO-terms enriched for the
651 upregulated and downregulated genes in Figure 2 and Supplemental Figure S3.

652

653 **Supplemental Dataset S3.** List of genes present in each cluster derived from PCA-SOM
654 analysis.

655

656 **Supplemental Dataset S4.** List of statistically significant GO-terms enriched for the genes
657 present in the PCA-SOM clusters.

658

659 **Supplemental Dataset S5.** List of cell cycle-related genes, transcription factors and leaf
660 developmental genes, and phytohormone-related genes present in clusters 1, 4, and 7 that were
661 used for generating heatmaps in figure 2, C-E and figure S3C.

662

663 **Supplemental Dataset S6.** List of genes present in the expression network shown in figure 2F
664 with their network properties and module belongings.

665

666 **Supplemental Dataset S7.** Normalized read counts used for generating gene coexpression
667 network.

668

669 **Acknowledgments**

670 V.J. and K.S. acknowledge their UGC-SRF and SERB-NPDF fellowships, respectively. We
671 thank the NIPGR Metabolomics Facility for Gibberellic Acid (GA) quantification and NIPGR
672 Central Instrumentation Facility for their support. Seeds of wild rice species and *Oryza*
673 *glaberrima* were kindly provided by Dr. Kuldeep Singh and Dr. Kumari Neelam, Punjab
674 Agricultural University, Ludhiana, India.

Tables

Table 1. Quantification of leaf length (cm) of fully-developed leaf two to leaf eight of the seven cultivated and four wild rice accessions. Each value represents mean ± SD, where n = 15 data points from different plants. Different letters indicate statistically significant differences according to one-way ANOVA followed by post-hoc Tukey HSD calculation at $P < 0.05$.

Oryza species	Cultivar/ accession number	Leaf number						
		Leaf 2	Leaf 3	Leaf 4	Leaf 5	Leaf 6	Leaf 7	Leaf 8
Oryza sativa ssp. japonica	Nipponbare	3.94 ± 0.35 (a)	11.8 ± 1.15 (a)	21.96 ± 1.53 (a)	26.92 ± 2 (a)	38.11 ± 1.73 (a)	44.37 ± 1.4 (a)	48.71 ± 2.84 (a)
Oryza sativa ssp. indica	IR 64	5.6 ± 0.22(b)	11.75 ± 0.85 (a)	20.95 ± 1.91 (a)	26.25 ± 1.72 (a)	34.05 ± 1.07 (a)	41.56 ± 1.48 (b)	44.85 ± 2.75 (b)
Oryza sativa ssp. indica	Vandana	4.54 ± 0.62 (a)	11.5 ± 1.43 (a)	21.12 ± 1.55 (a)	29.06 ± 1.34 (a)	32.59 ± 1.71 (b)	37.36 ± 1.77 (c)	45.59 ± 1.74 (ab)
Oryza sativa ssp. indica	Swarna	4.7 ± 0.44 (a)	14.93 ± 1.24 (b)	27.92 ± 2.52 (b)	39.88 ± 2.65 (b)	46.9 ± 1.87 (c)	52.76 ± 2.86 (d)	58.72 ± 3.03 (c)
Oryza sativa ssp. indica	Pusa Basmati1	6.25 ± 0.54(b)	14.66 ± 2.36 (b)	28.48 ± 3.11 (b)	37.11 ± 2.01 (c)	42.98 ± 1.76 (d)	48.3 ± 2.26 (a)	55.17 ± 1.94 (d)
Oryza sativa ssp. indica	Nagina 22	4.21 ± 0.38 (a)	14.55 ± 1.52 (b)	27.98 ± 1.3 (b)	38.5 ± 2.29 (bc)	44.56 ± 2.14 (de)	53.41 ± 2.59 (d)	62.77 ± 1.79 (e)
Oryza glaberrima	IR 102925	6 ± 0.3(b)	14.95 ± 1.65 (bc)	26.9 ± 1.18 (b)	38.2 ± 1.19 (c)	45.9 ± 2.42 (ce)	53.7 ± 2.4 (d)	59.5 ± 2.82 (c)
Oryza glumaepatula	IR104151	8.01 ± 0.56 (c)	23.24 ± 1.68 (e)	37.26 ± 3.1 (c)	43.3 ± 1.3 (d)	46.76 ± 1.51 (ce)	53.35 ± 2.05 (d)	63.91 ± 3.07 (e)
Oryza punctata	IRGC105137	6.08 ± 0.63(b)	17.67 ± 1.19 (cd)	34.38 ± 1.27 (cd)	47.52 ± 1.39 (e)	51.92 ± 1.31 (f)	58.26 ± 1.23 (e)	70.67 ± 2.04 (f)
Oryza latifolia	IRGC 99596	10.15 ± 0.62(d)	18.32 ± 1.42 (d)	31.52 ± 2.05 (d)	46.13 ± 1.19 (e)	53.12 ± 1.1 (f)	60.63 ± 2.26 (e)	70.93 ± 1.68 (f)
Oryza australiensis	IRGC 105272	20.57 ± 2.68 (e)	34.19 ± 3.44 (f)	50.66 ± 4.55 (e)	56.57 ± 2.6 (f)	64.74 ± 4.36 (g)	69.5 ± 0.71 (f)	87.8 ± 5.27 (g)

Table 2. Quantification of leaf kinematics parameters of the growing leaf four of selected cultivated and wild rice accessions. Each value represents mean ± SD (n = 15 for mature leaf length and leaf elongation rate, n = 5 for all other parameters). Different letters indicate statistically significant differences according to one-way ANOVA followed by post-hoc Tukey HSD calculation at $P < 0.05$.

Growth parameters	***O. sativa* cv. IR 64**	***O. sativa* cv. Nipponbare**	***O. glaberrima***	***O. australiensis***
Mature leaf length (cm)	20.06 ± 1.38(a)	21.46 ± 0.81(a)	26.98 ± 1.01(b)	41.38 ± 4.25(c)
Leaf elongation rate (mm/h)	1.32 ± 0.01(a)	1.34 ± 0.01(a)	2.01 ± 0(b)	2.41 ± 0.01(b)
Meristem length (mm)	7.52 ± 0.14(a)	7.81 ± 0.34(a)	12.32 ± 0.34(b)	16.66 ± 0.64(c)
Length of the growth zone (mm)	24 ± 1(a)	31.33 ± 0.58(b)	24.67 ± 1.53(a)	34.33 ± 0.58(c)
Mature cell length (µm)	70.61 ± 0.15(a)	64.26 ± 1.41(b)	66 ± 1.07(b)	84.57 ± 1.32(c)
Cell production rate (cells/h)	18.76 ± 0.12(a)	20.88 ± 0.4(b)	30.44 ± 0.51(c)	28.49 ± 0.42(d)
Number of cells in meristem	738.29 ± 27.5(a)	715.92 ± 17.05(a)	842.73 ± 31.5(b)	904.75 ± 52.9(b)
Number of cells in growth zone	1193.63 ± 70.37(a)	1328.8 ± 26.33(b)	1100.53 ± 43.44(ac)	1211.09 ± 38.48(abc)
Number of cells in elongation zone	455.35 ± 68.5(a)	612.88 ± 41.5(b)	257.8 ± 38.3(c)	306.34 ± 19.5(c)
Average cell division rate (cell. $cell^{-1}.h^{-1}$)	0.03 ± 0(a)	0.03 ± 0(ab)	0.04 ± 0(bc)	0.03 ± 0(ab)
Cell cycle duration (h)	27.29 ± 1.15(a)	23.78 ± 0.99(b)	19.2 ± 1.03(c)	22 ± 0.98(b)
Time in elongation zone (h)	24.26 ± 3.53(a)	29.34 ± 1.62(a)	8.47 ± 1.29(b)	10.76 ± 0.79(b)
Time in division zone (h)	260.01 ± 12.4(a)	225.54 ± 10.1(b)	186.66 ± 11.05(c)	216.13 ± 11.45(bc)
Length of cells leaving meristem (µm)	15.15 ± 0.37(a)	17.79 ± 0.41(a)	31.33 ± 1.41(b)	39.93 ± 3.36(c)
Average cell expansion rates (µm. $\mu m^{-1}.h^{-1}$)	0.06 ± 0.01(ac)	0.04 ± 0(a)	0.09 ± 0.01(bc)	0.07 ± 0.01(ac)

Figure Legends

Figure 1. Wild rice *Oryza australiensis* grows longer leaf compared to the selected cultivated rice accessions. A, Representative photographs of the selected cultivated and wild rice accessions showing leaf size variations. B, Quantification of mature leaf length of leaf two to leaf ten. C, Representative leaf four images at the second day of emergence. D, Quantification of leaf four lengths at the different day of emergence. E, Leaf elongation rate of the selected rice accessions. Values in graphs represent mean±SD (n=15). Different letters indicate statistically significant differences according to one-way ANOVA followed by post-hoc Tukey HSD at $P < 0.05$.

Figure 2. Transcriptome profiling reveals the key contribution of the cell cycle and Gibberellic Acid (GA) for differential leaf length across the selected rice accessions. A, Number of differentially expressed transcripts and enriched GO terms in *O. australiensis* compared to *O. sativa* cv. IR64 and *O. sativa* cv. Nipponbare. * show enriched GO terms. B, Gene expression clusters showing genotype-specific resolution for the selected four accessions derived from PCA-SOM analysis. Enriched GO terms are shown for *O. australiensis* and *O. glaberrima* specific clusters 1, 4, and 7. (C-E), Expression patterns of cell cycle-related genes (C), transcription factors and leaf developmental genes (D), and Gibberellic acid biosynthesis and signaling genes (E) present in clusters 1, 4 and 7 across the four accessions. F, Gene regulatory network generated for the genes from the relevant clusters of (B). Three different modules of the network are shown in different colors.
AUS= *O. australiensis,* GLA= *O. glaberrima,* IR= *O. sativa* cv. IR64, NIP= *O. sativa* cv. Nipponbare.

Figure 3. Leaf kinematics analyses confirm the cell division as a major regulator of rice leaf length. A, Different growth zones on leaf four of *O. sativa* cv. Nipponbare at the second day of emergence as quantified by epidermal cell length profiling and DAPI staining. B**,** Representative hand-drawn microscopic images of epidermal cells along with DAPI staining images for the different leaf-growth-zones of *O. sativa* cv. Nipponbare. C, Different growth zones on leaf four of *O. australiensis* at the second day of emergence. D, Representative hand-drawn microscopic images of epidermal cells along with DAPI staining images for the different

leaf-growth-zones of *O. australiensis.* Values in A and C represent mean±SD (n=5). Vertical lines of different colors represent the separation of different leaf-growth zones. White arrows in B and D show DAPI-stained nuclei indicating dividing cells. Red scale bar = 20μm in B and D.

Figure 4. GA-mediated cell division control regulates the rice leaf length. (A, B), Effect of GA3 (10μM) and Paclobutrazol (PAC, 1μM) treatments on leaf length of *O. sativa cv.* Nipponbare (A) and *O. australiensis* (B). Values represent mean±SD (n=15). Different letters indicate statistically significant differences at each day after emergence according to one-way ANOVA followed by post-hoc Tukey HSD calculation at $P < 0.05$. (C, D), GA quantification in leaf four of *O. sativa cv.* Nipponbare and *O. australiensis* at the second day of emergence. Data show mean ±SD (n=5),*** $P < 0.001$ by Student's t-test. (E, F), Different growth zones on leaf four of *O. sativa* cv. Nipponbare (E) and *O. australiensis* (F) in response to GA3 and PAC treatments as quantified by epidermal cell length profiling and DAPI staining. Values represent mean ±SD (n=5). Vertical lines of different colors represent the size of division zones under different treatments.

Figure 5. Zone-specific expression analysis of GA biosynthetic and signaling genes as well as cell cycle-related genes. (A-F), Expression pattern of GA biosynthesis genes *OsGA20OX2* and *OsGA3OX2* (A, B), genes encoding GRF transcription factors *OsGRF7* and *OsGRF8* (C, D), and cell cycle genes *OsCYCB1;4* and *OsCYCA3;2* (E, F) in two growth zones of *O. sativa cv.* Nipponbare and *O. australiensis.* Zone I represents the region from leaf base to 0.8cm and zone II represents 0.8cm to 1.6cm from the leaf base. (G-J), Effect of GA_3 treatment on the expression of *OsGRF7* (G), *OsGRF8* (H), *OsCYCB1;4* (I), and *OsCYCA3;2* (J) in the two growth zones of *O. sativa cv.* Nipponbare. Data shown are mean ±SD of three biological replicates, *** $P < 0.001$ by Student's t-test.

Figure 6. The silencing of GA-related genes confirms the GA-mediated regulation of rice leaf length. A, Shown are the leaf phenotypes of *OsGA20OX2* silencing in *O. sativa cv.* Nipponbare along with the control plants. B, Effect of *OsGA20OX2* silencing on leaf length

and size of division zone. C, Expression levels of target GA biosynthetic gene, *GRFs*, and *CYCLINs* in *OsGA20OX2* silencing lines. D, Shown are the leaf phenotypes of *OsGRF7* silencing in *O. sativa cv.* Nipponbare along with the control plants. E, Effect of *OsGRF7* silencing on leaf length and size of division zone. F, Expression analysis of target *GRF7* and *CYCLINs* in *OsGRF7* silencing lines. Data represent mean ±SD of at least three biological replicates, *** $P < 0.001$ and ** $P < 0.01$ by Student's t-test.

Figure 7. The GA-GRF-cell cycle module is a key regulator of the rice leaf length control. GA-mediated induction in the expression domain of GRF transcription factors expands the region with cyclin expression at the leaf base, thus promoting the longer division zone with a higher cell production rate leading to longer leaves in rice. Higher GA levels and downstream signaling resulting in increased cell division activity explained the longer leaves of the wild rice *O. australiensis* compared to the cultivated varieties.

Literature Cited

Achard P, Gusti A, Cheminant S, Alioua M, Dhondt S, Coppens F, Beemster GT, Genschik P (2009) Gibberellin signaling controls cell proliferation rate in Arabidopsis. Curr Biol **19:** 1188–1193

Andriankaja M, Dhondt S, De Bodt S, Vanhaeren H, Coppens F, De Milde L, Mühlenbock P, Skirycz A, Gonzalez N, Beemster GTS, et al. (2012) Exit from proliferation during leaf development in Arabidopsis thaliana: a not-so-gradual process. Dev Cell **22**: 64–78

Avramova, V, Sprangers, K, and Beemster, GTS (2015) The Maize Leaf: Another Perspective on Growth Regulation. Trends Plant Sci **20**: 787-797

Bar M, Ori N (2014) Leaf development and morphogenesis. Development **141**(22): 4219-30

Beemster GT, De Veylder L, Vercruysse S, West G, Rombaut D, Van Hummelen P, Galichet A, Gruissem W, Inze D, and Vuylsteke M (2005) Genome-wide analysis of gene expression profiles associated with cell cycle transitions in growing organs of Arabidopsis. Plant Physiol **138**: 734–743

Beltramino M, Ercoli M, Debernardi J, Goldy C, Rojas A, Nota F, Alvarez M, Vercruyssen L, Inzé D, Palatnik J, Rodriguez R (2018) Robust increase of leaf size by Arabidopsis thaliana GRF3-like transcription factors under different growth conditions. Sci Rep **8**: 13447

Chatterjee J, Dionora J, Elmido-Mabilangan A, Wanchana S, Thakur V, Bandyopadhyay A, Brar D, Quick W (2016) The evolutionary basis of naturally diverse rice leaves anatomy. PLoS ONE **11**: e0164532

Chen Q, Li W, Tan L, Tian F (2021) Harnessing knowledge from maize and rice domestication for new crop breeding. Mol Plant **14**: 9-26

Chen Y, Dan Z, Gao F, Chen P, Fan F, Li S (2020) Rice GROWTH-REGULATING FACTOR7 Modulates Plant Architecture through Regulating GA and Indole-3-Acetic Acid Metabolism. Plant Physiol **184** (1): 393-406

Chitwood D, Kumar R, Headland L, Ranjan A, Covington M, Ichihashi Y, Fulop D, Jiménez-Gómez J, Peng J, Maloof J, Sinha N (2013) A quantitative genetic basis for leaf morphology in a set of precisely defined tomato introgression lines. Plant Cell **25**: 2465–2481

Chitwood DH, Sinha NR (2016) Evolutionary and environmental forces sculpting leaf development. Curr Biol **26**(7): 297-306

Choi J, Kende H (2004) Whole genome analysis of the OsGRF gene family encoding plant-specific putative transcription activators in rice (*Oryza sativa* L.). Plant Cell Physiol **45**: 897-904

Csardi G, Nepusz T (2006) The igraph software package for complex network research. InterJournal, Complex Systems **1695**: 1–9

Davière JM, Achard P (2013) Gibberellin signaling in plants. Development **140**: 1147-51

Du F, Guan C, Jiao Y (2018) Molecular mechanisms of leaf morphogenesis. Mol Plant **11**(9): 1117-1134

Efroni I, Eshed Y, Lifschitz E (2010) Morphogenesis of simple and compound leaves: a critical review. Plant Cell **4**: 1019-32

Fina J, Casadevall R, AbdElgawad H, Prinsen E, Markakis M, Beemster G, Casati P (2017) UV-B Inhibits Leaf Growth through Changes in Growth Regulating Factors and Gibberellin Levels. Plant Physiol **174**(2): 1110-1126

Gonzalez N, De Bodt S, Sulpice R, Jikumaru Y, Chae E, Dhondt S, Van Daele T, De Milde L, Weigel D, Kamiya Y, Stitt M, Beemster GT, Inzé D (2010) Increased leaf size: different means to an end. Plant Physiol **153**: 1261-79

Gonzalez N, Vanhaeren H, Inzé D (2012) Leaf size control: complex coordination of cell division and expansion. Trends Plant Sci **6**: 332-40

Granier C, Tardieu F (2009) Multi-scale phenotyping of leaf expansion in response to environmental changes: the whole is more than the sum of parts. Plant Cell Environ **32**: 1175-1184

Huang X, Kurata N, Wei X, Wang ZX, Wang A, Zhao Q, Zhao Y, Liu K, Lu H, Li W, et al. (2012) A map of rice genome variation reveals the origin of cultivated rice. Nature **490**: 497–501

Inze D, De Veylder L (2006) Cell cycle regulation in plant development. Annu Rev Genet **40**: 77–105

Jones R, Kaufman P (1983) The role of gibberellins in plant cell elongation. Critical Reviews in Plant Sciences **1**: 23-47

Kalve S, de Vos D, Beemster GTS (2014) Leaf development: a cellular perspective. Front Plant Sci **5**: 362

Kant R, Dasgupta I (2017) Phenotyping of VIGS-mediated gene silencing in rice using a vector derived from a DNA virus. Plant Cell Rep **36**(7): 1159-1170

Kierzkowski D, Runions A, Vuolo F, Strauss S, Lymbouridou R, Routier-Kierzkowska AL, Wilson-Sánchez D, Jenke H, Galinha C, Mosca G, Zhang Z, Canales C, Dello Ioio R, Huijser P, Smith RS, Tsiantis M (2019) A Growth-Based Framework for Leaf Shape Development and Diversity. Cell **177**(6): 1405-1418

Kim J, Choi D, Kende H (2003) The AtGRF family of putative transcription factors is involved in leaf and cotyledon growth in Arabidopsis. Plant J **36**: 94–104

van der Knaap E, Kim J, Kende H (2000) A novel gibberellin-induced gene from rice and its potential regulatory role in stem growth. Plant Physiol **122**(3): 695-704

Langfelder P, Horvath S (2008) WGCNA: an R package for weighted correlation network analysis. BMC Bioinformatics **9**: 559

Langmead B, Salzberg S (2012) Fast gapped-read alignment with Bowtie 2. Nat Methods **9** (4): 357-9

Lantzouni O, Alkofer A, Falter-Braun P, Schwechheimer C (2020) GROWTH-REGULATING FACTORS Interact with DELLAs and Regulate Growth in Cold Stress. Plant Cell **32**(4): 1018-1034

Li H, Handsaker B, Wysoker A, Fennell T, Ruan J, Homer N, Marth G, Abecasis G, Durbin R (2009) 1000 Genome Project Data Processing Subgroup, The Sequence Alignment/Map format and SAMtools. Bioinformatics **25**(16): 2078–2079

Li LC, Kang DM, Chen ZL, Qu LJ (2007) Hormonal Regulation of Leaf Morphogenesis in *Arabidopsis*. J Integr Plant Biol **49**: 75-80

Li S, Tian Y, Wu K, Ye Y, Yu J, Zhang J, Liu Q, Hu M, Li H, Tong Y, Harberd N, Fu X (2018) Modulating plant growth-metabolism coordination for sustainable agriculture. Nature **560**(7720): 595-600

Livak KJ, Schmittgen TD (2001) Analysis of relative gene expression data using real-time quantitative PCR and the 2(-Delta Delta C(T)) Method. Methods **25**(4): 402-8

Longeman J, Schell J, Willmitzer L (1987) Improved method for the isolation of RNA from plant tissues. Analytical Biochemistry **163**: 16–20

Mathan J, Singh A, Ranjan A (2021) Sucrose transport and metabolism control carbon partitioning between stem and grain in rice. J Exp Bot erab066, https://doi.org/10.1093/jxb/erab066

Nelissen H, Eeckhout D, Demuynck K, Persiau G, Walton A, van Bel M, Vervoort M, Candaele J, De Block J, Aesaert S, et al (2015) Dynamic changes in ANGUSTIFOLIA3

complex composition reveal a growth regulatory mechanism in the maize leaf. Plant Cell **27**: 1605–1619

Nelissen H, Rymen B, Jikumaru Y, Demuynck K, Van Lijsebettens M, Kamiya Y, Inzé D, Beemster GTS (2012) A local maximum in gibberellin levels regulates maize leaf growth by spatial control of cell division. Curr Biol **22**: 1183–1187

Nelissen H, Sun X, Rymen B, Jikumaru Y, Kojima M, Takebayashi Y, Abbeloos R, Demuynck K, Storme V, Vuylsteke M, De Block J, Herman D, Coppens F, Maere S, Kamiya Y, Sakakibara H, Beemster G and Inzé D (2018) The reduction in maize leaf growth under mild drought affects the transition between cell division and cell expansion and cannot be restored by elevated gibberellic acid levels. Plant Biotechnol J **16**: 615-627

Omidbakhshfard MA, Proost S, Fujikura U, Mueller-Roeber B (2015) Growth-Regulating Factors (GRFs): A Small Transcription Factor Family with Important Functions in Plant Biology. Mol Plant **8**: 998-1010.

Patel RK, Jain M (2012) NGS QC Toolkit: A Toolkit for Quality Control of Next Generation Sequencing Data. PLoS ONE **7**(2): e30619

Piazza P, Jasinski S, Tsiantis M (2005) Evolution of leaf developmental mechanisms. New Phytol **167**: 693–710

Robinson M, McCarthy D, Smyth G (2010) edgeR: a Bioconductor package for differential expression analysis of digital gene expression data. Bioinformatics **26**(1): 139–140

Rodriguez RE, Debernardi JM, Palatnik JF (2013) Morphogenesis of simple leaves: regulation of leaf size and shape. Wiley Interdiscip Rev Dev Biol **3**(1): 41-57

Sanchez PL, Wing RA, and Brar DS (2013) The Wild Relative of Rice: Genomes and Genomics. In: Zhang Q and Wing RA (eds.) Plant Genetics and Genomics: Crops and Models 5 Genetics and Genomics of Rice, Springer, New York, 2–25

Sarvepalli K, Das Gupta M, Challa KR, Nath U (2019) Molecular cartography of leaf development - role of transcription factors. Curr Opin Plant Biol **47**: 22-31

Spielmeyer W, Ellis MH and Chandler PM (2002) Semidwarf (sd-1), ‘‘green revolution” rice, contains a defective gibberellin 20-oxidase gene. Proc Natl Acad Sci USA **99**: 9043–9048

Sprangers K, Avramova V, Beemster GT (2016) Kinematic Analysis of Cell Division and Expansion: Quantifying the Cellular Basis of Growth and Sampling Developmental Zones in Zea mays Leaves. J Vis Exp **118**: 54887

Su YH, Liu YB, Zhang XS (2011) Auxin-cytokinin interaction regulates meristem development. Mol Plant **4**: 616-25

Takatsuka H, Umeda M (2014) Hormonal control of cell division and elongation along differentiation trajectories in roots. J Exp Bot **65**: 2633–2643

Tardieu F, Granier C (2000) Quantitative analysis of cell division in leaves: methods, developmental patterns and effects of environmental conditions. Plant Mol Biol **43**: 555-67

Tardieu F, Reymond M, Hamard P, Granier C, Muller B (2000) Spatial distributions of expansion rate, cell division rate and cell size in maize leaves: a synthesis of the effects of soil water status, evaporative demand and temperature. J Exp Bot **51**: 1505-1514

Tian F, Yang DC, Meng YQ, Jin JP and Gao G (2019) PlantRegMap: charting functional regulatory maps in plants. Nucleic Acids Res **48**(D1): D1104-D1113

Townsley BT, Sinha NR (2012) A new development: evolving concepts in leaf ontogeny. Annu Rev Plant Biol **63**: 535-62

Vercruysse J, Baekelandt A, Gonzalez N, Inzé D (2020b) Molecular networks regulating cell division during Arabidopsis leaf growth. J Exp Bot **71**(8): 2365-2378

Vercruysse J, van Bel M, Osuna-Cruz CM, Kulkarni SR, Storme V, Nelissen H, Gonzalez N, Inzé D, Vandepoele K (2020a) Comparative transcriptomics enables the identification of functional orthologous genes involved in early leaf growth. Plant Biotechnol J **2**: 553-567

Wehrens R, Buydens L (2007) Self- and super-organizing maps in R: the Kohonen package. J Stat Softw **21**: 1–19

Willige B, Ghosh S, Nill C, Zourelidou M, Dohmann E, Maier A, Schwechheimer C (2007) The DELLA domain of GA INSENSITIVE mediates the interaction with the GA INSENSITIVE DWARF1A gibberellin receptor of Arabidopsis. Plant Cell **19**(4): 1209–1220

Wu L, Zhang D, Xue M, Qian J, He Y and Wang S (2014) Overexpression of the maize GRF10, an endogenous truncated GRF protein, leads to reduction in leaf size and plant height. J Integr Plant Biol **56**: 1053-1063

Zhu X, Long S, Ort DR (2010) Improving photosynthetic efficiency for greater yield. Annu Rev Plant Biol **61**: 235-261